THE JOURNAL OF PHYSICAL CHEMISTRY Letters

Letter

pubs.acs.org/JPCL

Singlet Fission in Weakly Interacting Acene Molecules

Sharareh Izadnia,[†] David W. Schönleber,[‡] Alexander Eisfeld,[‡] Alexander Ruf,[†] Aaron C. LaForge,*[,†] and Frank Stienkemeier[†]

[†]Physikalisches Institut, Universität Freiburg, 79104 Freiburg, Germany

[‡]Max Planck Institute for the Physics of Complex Systems, 01187 Dresden, Germany

Supporting Information

ABSTRACT: The energy conversion in solar cells has conventionally been limited by the Shockley–Queisser limit. Singlet fission (SF), a decay mechanism where a single excited singlet state is converted into two triplet states, can drastically improve this efficiency. For the most part, observation of SF has been limited to crystalline structures in solids and films, where strong ordering was present. Here we report on singlet fission in a disordered system where organic chromophores are distributed on the surface of a rare gas cluster. In this case, the intermolecular distances and degree of excitation can be varied to obtain their effects on the rate of singlet fission. We introduce a kinematic model that takes into account the details of the geometrical arrangement of the system as well as the time-dependent populations of the relevant states of each molecule and evaluate the trends obtained by SF on the experimental observables.

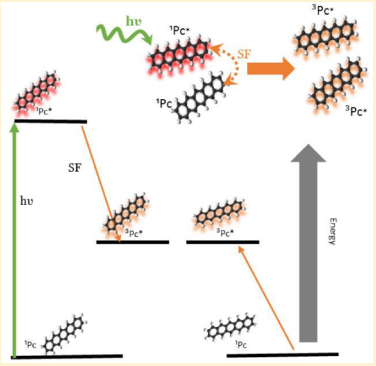

To overcome the energy conversion limitations of single junction solar cells, photovoltaic research has typically focused on multilayered junctions to broaden the wavelength range of absorbed light. Organic photovoltaics, on the contrary, not only offer a low-cost alternative to the their inorganic counterparts but also provide new processes that can overcome the limitations set by Shockley and Queisser.[1] Singlet fission (SF), for instance, can directly surmount the limitation that a single electron–hole pair is produced per photon absorbed, and its ability to enhance the quantum efficiency of solar cells has already been demonstrated.[2−4] In the SF process, one molecule is initially in a singlet excited state and a (nearby) molecule in the ground state; after the SF process, both molecules are in their triplet excited states (cf. Figure 2iii). SF has been observed in condensed systems (thin films and crystals) for over 50 years.[5,6] Despite its important consequences in applied research, the exact mechanisms of SF are still not completely understood. Excitonic coupling and long-range order have long been considered essential for SF.[7−10] However, recently, SF has been observed in an amorphous solid,[11] a solution,[12] and even intramolecularly in covalently linked pentacene molecules,[13,14] which strongly suggest that ordering is not an absolute necessity.

Here we perform a systematic study on acene (anthracene (Ac), tetracene (Tc), and pentacene (Pc)) -doped rare gas clusters specifically in the region where nonradiative decay mechanisms such as SF become significant. Acene molecules are particularly well-suited to studying SF as the process goes from being energetically forbidden (Ac) to energetically allowed for the larger polyacenes. To form a collective ensemble of molecules that can be well-characterized by spectroscopic means and where perturbation of the molecules by the environment is minimized, we isolate acene molecules on rare gas clusters. Molecules attached to the surface of rare gas clusters offer a unique medium to study their composition[15] because the electronic, vibrational, and rotational excitations can be much better resolved than in materials in the condensed phase. The molecular arrangement is considered highly disordered compared with crystals or thin films, and it is possible to apply a large amount of experimental control to the system (e.g., average intermolecular distances, number of excited molecules).

Our experiments show significant differences between Pc/Tc-doped rare gas clusters compared with Ac-doped clusters, which we attribute to SF. This conclusion is supported by numerical simulations, where we use a novel geometry-specific model for the population dynamics, suitable for small, disordered systems.

Figure 1a shows the fluorescence lifetimes of Ac (black squares), Tc (red circles), and Pc (blue triangles) as a function of the mean number of molecules attached to the surface of neon clusters (top axis as a function of the mean intermolecular distance). The mean cluster size was $n \approx 122\,000$ atoms (diameter ∼17 nm). The laser was tuned to the electronic S_0–S_1 transition (27 536 (Ac), 22 208 (Tc) and 18 447 (Pc) cm^{-1}). A power density of 8 kW/cm^2 for Tc/Pc and 3 kW/cm^2 for Ac was used such that the laser-induced fluorescence (LIF) intensity was maximized while avoiding any signs of saturation. Unless otherwise noted, these experimental parameters were used throughout the measurements. As the number of attached

Received: February 9, 2017
Accepted: April 19, 2017
Published: April 19, 2017

DOI: 10.1021/acs.jpclett.7b00319
J. Phys. Chem. Lett. 2017, 8, 2068–2073

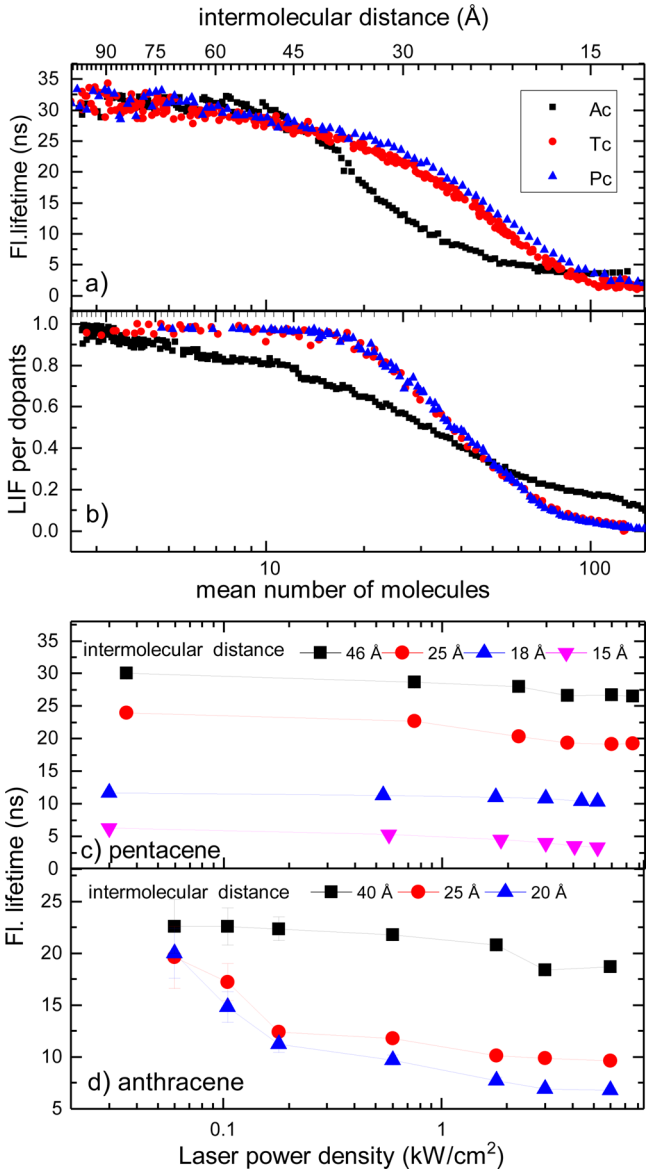

Figure 1. (a) Fluorescence lifetime and (b) normalized LIF intensity per molecule of Ac (black squares), Tc (red circles), and Pc (blue triangles) on neon clusters as a function of the mean number of attached molecules (top axis as a function of the mean intermolecular distance) for a power density of 8 kW/cm^2 for Tc/Pc and 3 kW/cm^2 for Ac. The fluorescence lifetime as a function of the laser power for different intermolecular distances is shown for (c) Pc and (d) Ac. The neon clusters to which the acene molecules are attached have an average size $n \approx 122\,000$ atoms.

molecules is increased, a noticeable reduction is observed in the fluorescence lifetime, asymptotically approaching 2 ns for Tc and Pc and 3.5 ns for Ac. As was previously reported, no apparent features (e.g., lineshifts or additional broadening) were observed in the LIF spectra for higher doping numbers; therefore agglomerated molecules with strong interactions do not contribute to the signals discussed here.[16] Thus the lifetime reduction is considered to be a cooperative effect due to weak, long-range interactions between the attached chromophores.

The lifetime reduction could be due to an increase in the radiative decay rate, that is, superradiance,[16] but could also be due to nonradiative processes. To distinguish the underlying mechanism, we plot in Figure 1b the normalized LIF intensity per attached molecule as a function of the mean number of attached molecules. For the case that nonradiative processes are not allowed, an increased number of excited molecules results in an increased LIF intensity; in other words, each photon absorbed results in a fluorescent photon being emitted, and thus the LIF per dopant is equal to 1. Nonradiatave processes, in contrast, can result in a loss of LIF intensity or quantum efficiency. As can be seen in Figure 1b, Ac shows a decrease in the LIF intensity per molecule already for a small number of attached molecules. As such, it is clear that nonradiative losses such as intersystem crossings[17] and exciton−exciton annihilation are always present for the case of Ac. For Tc and Pc, on the contrary, the intensity remains constant until ∼20 attached molecules, indicating that there are no additional nonradiative processes. Because Tc and Pc show in this range already a lifetime reduction, we attribute this reduction to superradiance, as discussed in a previous publication.[16] For higher doping numbers, the LIF intensity decreases, which we attribute to the onset of nonradiative effects, and because this effect becomes stronger when many dopants are attached, it is reasonable to conclude that this is due to the decrease in intermolecular distance.

To further elucidate the mechanisms of lifetime reduction, it is helpful to differentiate those brought on by multiple excitations (e.g., superradiance) from those due to the presence of additional molecules (e.g., SF). We have thus varied both the number of dopants (thereby varying the average intermolecular distance) as well as the laser power (0.03−10 kW/cm^2, thereby varying the number of excitations in the ensemble). Figure 1c,d shows the fluorescence lifetime as a function of the laser power for different intermolecular distances of Pc- and Ac-doped Ne clusters, respectively. Because Tc and Pc show a nearly identical behavior, we only show the results for Pc and Ac. For all acenes, a reduction in lifetime is observed for increasing laser power. In the case of Pc/Tc, this is attributed to an increased number of excited chromophores which de-excite via superradiance while for Ac, nonradiative processes such as exciton−exciton annihilation can additionally contribute to the lifetime reduction. For low laser powers, at most one molecule is excited, thereby excluding any effect of superradiance. (At 0.03 kW/cm^2, the probability of one molecule being excited is 25%.) In this regime, there are stark differences between Pc/Tc and Ac. For Pc, the fluorescence lifetime decreases dramatically for small intermolecular distances even at the lowest laser power. For an average intermolecular distance of 15 Å, the lifetime is roughly six times smaller than the lifetime for larger intermolecular distance. For Ac, no such dependence is observed, and all intermolecular distances converge to the same fluorescence lifetime at low laser power. As such, the lifetime reduction observed for Pc is attributed to SF which is energetically forbidden in Ac.

To gain more insight into the contributions of the different fluorescence lifetime-reducing processes, a detailed theoretical model is needed in which their respective effects can be systematically investigated. Previous approaches[11,19−21] employed effective rate equation models considering only one or two effective singlet and triplet states, neglecting, in particular, the ground state. In general, because of the relatively strong laser power, the inclusion of the ground-state population is crucial because the ground-state population should *not* be assumed to remain unaffected during the excitation process. Therefore, we model ground, triplet, and singlet population of the individual molecules in our rate equation. Furthermore,

DOI: 10.1021/acs.jpclett.7b00319
J. Phys. Chem. Lett. 2017, 8, 2068−2073

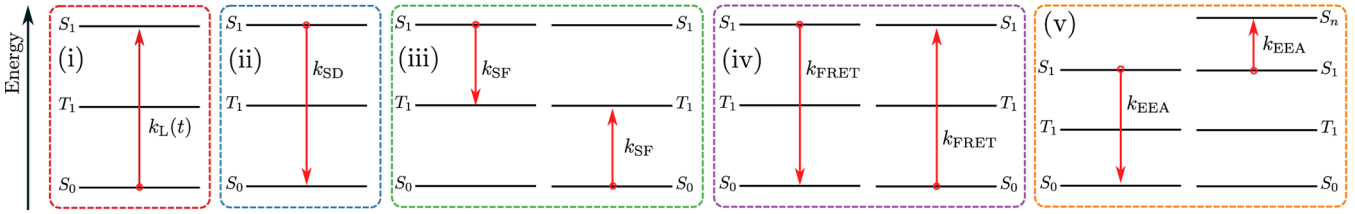

Figure 2. Sketch of the processes included in our numerical simulation: (i) laser excitation, (ii) radiative decay, (iii) singlet fission, (iv) singlet hopping, and (v) exciton−exciton annihilation (EEA). (iii−v) Nonradiative processes. In SF (iii), a singlet excitation is converted into two triplet excited states located on neighboring molecules. In singlet hopping (iv), a singlet and a ground-state molecule swap their states according to Förster resonance energy transfer (FRET). In EEA (v), one of two singlet-excited molecules is excited to a higher state, while the other is de-excited to the ground state, followed by an internal conversion process, which brings the higher excited molecule back to its first excited singlet state.[18]

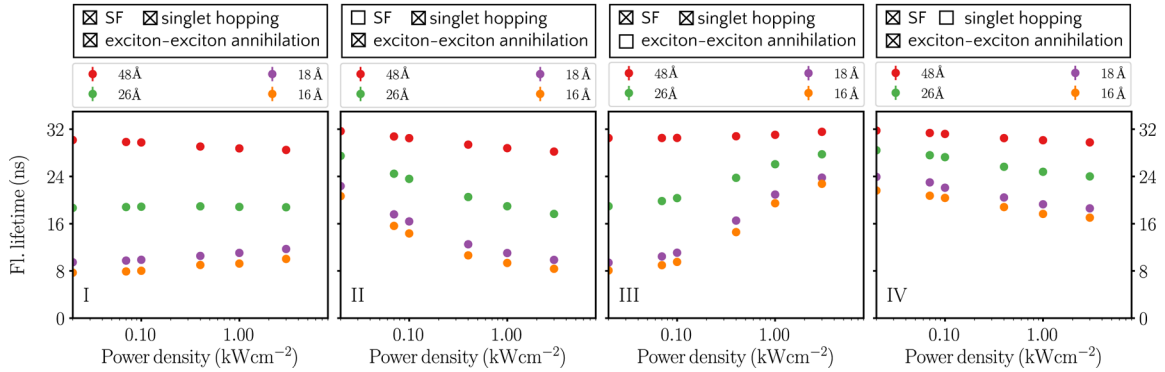

Figure 3. Fluorescence lifetime as a function of the laser power density for different numbers of molecules corresponding to different mean intermolecular distances. In different columns, different nonradiative processes are accounted for (see top box). Parameters are k_{SD} = 1/33 ns^{-1}, k_{SF} = 0.2 ns^{-1}, d_{SF} = 2.5 nm, and k_{EEA} = 64 ns^{-1} nm^6.

unlike in previous models, in our modeling, rates corresponding to nonradiative processes explicitly depend on the geometrical details of the molecules' arrangement, which we take to be random on the cluster.

In the following, we discuss the main processes of our theoretical model; the details can be found in the Supporting Information. The included processes are sketched in Figure 2. Laser excitation to the singlet state is modeled by a time-dependent excitation rate $k_L(t)$. To account for strongly bound complexes that cannot be optically excited, we introduce a distance $R_{complex}$ = 1.2 nm and exclude all molecules with intermolecular distances smaller than $R_{complex}$ from the excitation process and the subsequent dynamics. We describe radiative decay of a molecule from its singlet state to its ground state using a rate k_{SD}, taken to be independent of the number of excited molecules. For singlet fission we employ a crude ad hoc modeling because the microscopic details of SF are not yet understood. Specifically, we assume that SF occurs with a rate k_{SF} if a molecule in its ground state is within a certain distance d_{SF} to a singlet-excited molecule. The SF rate and radius thus give an effective/coarse-grained description of SF, which may be facilitated by processes not included in the modeling, such as molecular diffusion. We account for singlet hopping by a hopping rate k_{FRET} that depends on distances and orientations of the transition dipoles of the molecules.[22,23] We model exciton−exciton annihilation (EEA) using a rate k_{EEA} that scales the distance and orientation dependence of the EEA process. This dependence is assumed to be the same as that used for singlet hopping.

In Figure 3 we show exemplary model simulations of the fluorescence lifetime as a function of laser power density for different mean intermolecular distances. A combination of all nonradiative processes, namely, SF, singlet hopping, and EEA, is displayed in Figure 3I; Figure 3II−IV shows calculations in which each individual nonradiative process is turned off. In the presence of all nonradiative processes (Figure 3I), the fluorescence lifetime strongly depends on the mean intermolecular distance and, in particular, decreases with decreasing intermolecular distance, while the dependence of the fluorescence lifetime on the laser power is weak. When we set the SF rate k_{SF} = 0 (shown in Figure 3II), the dependence of fluorescence lifetime on intermolecular distance becomes much weaker for low laser powers; that is, for the same intermolecular distance the fluorescence lifetimes increase as compared with Figure 3I. For high laser powers, no pronounced changes occur. Conversely, when we set the EEA rate k_{EEA} = 0 (shown in Figure 3III), for high laser powers the fluorescence lifetimes increase when compared with the fluorescence lifetimes at same intermolecular distance in Figure 3I, while at low laser powers no pronounced changes occur. When we do not include singlet hopping in our simulations (as shown in Figure 3IV), the dependence of fluorescence lifetimes on intermolecular distance becomes weaker for all laser powers; the fluorescence lifetimes increase, however, slightly more for low laser powers.

These trends in the dependence of fluorescence lifetime on laser power and mean intermolecular distance do not show a strong dependence on the chosen rates for the nonradiative processes. Nevertheless, we have chosen the rates in Figure 3 so as to allow for comparison with experiment: k_{SD} is taken as the inverse single-molecule lifetime of Pc/Tc; the singlet hopping rate k_{FRET} is calculated from FRET theory[23] using the dipole moment of Pc. The exciton−exciton annihilation rate k_{EEA} is comparable to the rate obtained from measurements in Pc

DOI: 10.1021/acs.jpclett.7b00319
J. Phys. Chem. Lett. 2017, 8, 2068−2073

films.[24] As previously discussed, the SF rate k_{SF} resulting from our model is specific to the considered system without long-range order and hence does not allow for direct comparison to rates observed in crystals or thin films.

We now compare Figure 3 with the corresponding experimental data shown Figure 1c,d. (See the Supporting Information for a comparison of our simulation results with experimental data for the observables shown in Figure 1a,b.) To obtain a similar dependence of the fluorescence lifetimes on intermolecular distance and laser power as measured for Pc, namely, a strong dependence of fluorescence lifetimes on intermolecular distance but a weak dependence on laser power, we need to include all nonradiative processes in our simulation (cf. Figure 1c and Figure 3I). In contrast, the weak dependence of fluorescence lifetimes on intermolecular distance at low laser powers observed in experiment for Ac, where SF is energetically forbidden, is captured in our simulations for zero SF rate (cf. Figure 1d and Figure 3II). We hence conclude that SF is a prominent decay mechanism for both Pc and Tc, while it is not observed in Ac. For the case of Pc/Tc, this would mean that for weakly bound, disordered systems SF is energetically allowed.

The interpretation of the experimental trends in terms of SF processes could be directly confirmed by experimentally detecting the triplet state population at later times after singlet excitation. In condensed systems, it is possible to perform transient absorption spectroscopy to probe the state of the system (e.g., refs 8 and 11−14); however, for a dilute system (e.g., supersonic gas jets) such as ours, this technique is not possible. We have therefore employed a pump−probe technique as a means to investigate the evolution of excited states. After a delay of ∼75 ns the initial excitation pulse is back-reflected as a probe pulse into the interaction region. The long delay time is necessary to completely isolate singlet-fluorescence of the pump pulse from the probe pulse. Because of the long lifetime of the triplet state, a molecule in the triplet state cannot be re-excited by a subsequent laser pulse and is therefore considered to be in a dark state. If the molecule relaxes to the ground state, then, conversely, the probe pulse can re-excite the molecule to the singlet state. In this way, in principle, we can probe whether population returns to the singlet ground state or if long-lived, triplet states are populated. An exemplary time-dependent LIF intensity is given in the inset of Figure 4. Typically, the probe pulse is roughly half the intensity of the pump pulse due to photoabsorption and optical losses. The intensity as a function of a parameter that varies the SF rate should clearly show the population of triplets by a decreasing ratio. The ratio of the integrated LIF signal of the probe pulse (pulse 2) to the pump pulse (pulse 1) as a function of the mean number of attached dopants is shown in Figure 4. In the case of Pc, the integrated ratio remains constant for fewer than 20 molecules; increasing the number of dopants further, the ratio then decreases to about half its size. A mean number of 20 molecules attached corresponds to an average intermolecular distance where nonradiative processes such as SF become prominent. Therefore, one can conclude that for small intermolecular distances nonradiative processes play a strong role and a large number of molecules have undergone SF. In contrast, Ac shows a completely different behavior; the integrated ratio is relatively unchanged by increasing the number of attached molecules. Accordingly, it appears that Ac has most likely relaxed back to the ground state, leading to an additional photon absorbed; however, our theoretical model has been unable to reproduce such behavior.

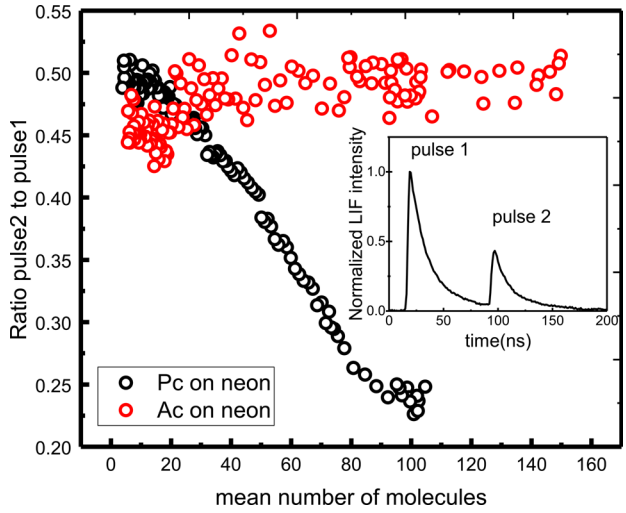

Figure 4. Integrated LIF ratio, pulse 2 to pulse 1, as a function of the mean number of attached molecules, Pc (black circles) or Ac (red circles), to the surface of neon clusters of size $n \approx 122\,000$ atoms and a power density of 8 kW/cm^2 for Pc and 3 kW/cm^2 for Ac. Inset: normalized LIF intensity spectrum. The double pulsing scheme is described in detail in the text.

In summary, the combined experimental and theoretical study strongly suggests that SF is an active decay mechanism in a disordered system where long-range interaction and strongly bound structure/ordering is not necessary. In this case, SF was observed for Pc/Tc-doped Ne clusters while unseen for Ac-doped Ne clusters. By varying different parameters and comparing experimental observables with theory, we can better distinguish the system dynamics and characterize individual decay processes. Microscopic modeling offers a novel means to analyze SF experiments in disordered systems. More knowledge on the geometry as well as the geometry dependence of the various nonradiative processes is necessary for the refinement of a microscopic model such as the one employed here. Pump−probe measurements confirm SF by indicating the population of long-lived triplet states. In general, the observation of SF in a disordered systems is encouraging for the prospect of SF-based organic photovoltaics, and, as an outlook, we wish to extend our studies to new organic molecules with lesser known excitation schemes in addition to directly measuring the triplet state population.

EXPERIMENTAL METHODS

The experimental setup of the molecular beam apparatus has previously been described in detail;[25,26] therefore, only a brief description is given. The neon cluster beam was created by supersonic expansion of high pressure, cryogenically cooled rare gas through an Even Lavie pulsed nozzle with an aperture diameter of 60 μm.[27] According to scaling laws[28−30] and recently performed titration measurements,[31] the mean size of the neon cluster was estimated to be between 18 000 and 15 0000 atoms depending on the temperature and pressure in the nozzle. The cluster beam has an approximate pulse length of 30 μs at 200 Hz repetition rate with a temperature of 10 ± 4 K.[32,33] After the neon clusters were formed, acene molecules were evaporated in a doping cell and attached to the surface of the cluster by inelastic collisions (pick-up method).[34] The mean number of molecules attached to the cluster was determined by the neon cluster size and the molecular partial pressure in

DOI: 10.1021/acs.jpclett.7b00319
J. Phys. Chem. Lett. 2017, 8, 2068−2073

doping cell.[35,36] Next, the acene-doped neon clusters were excited by a tunable dye laser (Sirah Cobra) with a temporal width of 9 ns, which was pumped by a pulsed Nd:YLF laser (Edgewave IS-IIIE). To cover the necessary spectral ranges of 22 000−23 200 and 18 000−19 000 cm^{-1}, Coumarin 2 and 157 were used as laser dyes, respectively while to cover the frequency range of 27 000−28 000 cm^{-1}, Pyredin 2 was used in combination with a frequency doubling unit. The photons generated by LIF were collected by a lens doublet and detected on a photomultiplier tube (Hamamatsu R 5600U-01) placed perpendicular to both the neon cluster and laser beam. Finally, flux and doping conditions of the cluster beam were analyzed downstream by a quadrupole mass spectrometer (EXTREL Max 1000).

■ ASSOCIATED CONTENT

Supporting Information

The Supporting Information is available free of charge on the ACS Publications website at DOI: 10.1021/acs.jpclett.7b00319.

Detailed description of the theoretical modeling: algorithm for distributing molecules on the cluster, rate equation, distance and orientation dependence of the nonradiative processes' rates, additional simulation results, fit of the fluorescence lifetime, and connection between mean intermolecular distance and dopant number. (PDF)

■ AUTHOR INFORMATION

Corresponding Author

*E-mail: aaron.laforge@physik.uni-freiburg.de.

ORCID

Alexander Eisfeld: 0000-0001-9645-440X

Aaron C. LaForge: 0000-0002-5758-6917

Notes

The authors declare no competing financial interest.

■ ACKNOWLEDGMENTS

We thank M. Walter and C. Bentley for helpful discussions. A.C.L. gratefully acknowledges support from Carl-Zeiss-Stiftung.

■ REFERENCES

(1) Shockley, W.; Queisser, H. J. Detailed Balance Limit of Efficiency of p-n Junction Solar Cells. *J. Appl. Phys.* **1961**, *32*, 510−519.

(2) Reusswig, P. D.; Congreve, D. N.; Thompson, N. J.; Baldo, M. A. Enhanced External Quantum Efficiency in an Organic Photovoltaic Cell via Singlet Fission Exciton Sensitizer. *Appl. Phys. Lett.* **2012**, *101*, 113304.

(3) Jadhav, P. J.; Brown, P. R.; Thompson, N.; Wunsch, B.; Mohanty, A.; Yost, S. R.; Hontz, E.; Van Voorhis, T.; Bawendi, M. G.; Bulović, V.; et al. Triplet Exciton Dissociation in Singlet Exciton Fission Photovoltaics. *Adv. Mater.* **2012**, *24*, 6169−6174.

(4) Congreve, D. N.; Lee, J.; Thompson, N. J.; Hontz, E.; Yost, S. R.; Reusswig, P. D.; Bahlke, M. E.; Reineke, S.; Van Voorhis, T.; Baldo, M. A. External Quantum Efficiency Above 100% in a Singlet-Exciton-Fission−Based Organic Photovoltaic Cell. *Science* **2013**, *340*, 334−337.

(5) Smith, M. B.; Michl, J. Singlet Fission. *Chem. Rev.* **2010**, *110*, 6891−6936.

(6) Smith, M. B.; Michl, J. Recent Advances in Singlet Fission. *Annu. Rev. Phys. Chem.* **2013**, *64*, 361−386.

(7) Johnson, J. C.; Nozik, A. J.; Michl, J. The Role of Chromophore Coupling in Singlet Fission. *Acc. Chem. Res.* **2013**, *46*, 1290−1299.

(8) Chan, W.-L.; Ligges, M.; Jailaubekov, A.; Kaake, L.; Miaja-Avila, L.; Zhu, X.-Y. Observing the Multiexciton State in Singlet Fission and Ensuing Ultrafast Multielectron Transfer. *Science* **2011**, *334*, 1541−1545.

(9) Zimmerman, P. M.; Bell, F.; Casanova, D.; Head-Gordon, M. Mechanism for Singlet Fission in Pentacene and Tetracene: From Single Exciton to Two Triplets. *J. Am. Chem. Soc.* **2011**, *133*, 19944−19952.

(10) Zimmerman, P. M.; Zhang, Z.; Musgrave, C. B. Singlet Fission in Pentacene through Multi-Exciton Quantum States. *Nat. Chem.* **2010**, *2*, 648−652.

(11) Roberts, S. T.; McAnally, R. E.; Mastron, J. N.; Webber, D. H.; Whited, M. T.; Brutchey, R. L.; Thompson, M. E.; Bradforth, S. E. Efficient Singlet Fission Discovered in a Disordered Acene Film. *J. Am. Chem. Soc.* **2012**, *134*, 6388−6400.

(12) Walker, B. J.; Musser, A. J.; Beljonne, D.; Friend, R. H. Singlet Exciton Fission in Solution. *Nat. Chem.* **2013**, *5*, 1019−1024.

(13) Sanders, S. N.; Kumarasamy, E.; Pun, A. B.; Trinh, M. T.; Choi, B.; Xia, J.; Taffet, E. J.; Low, J. Z.; Miller, J. R.; Roy, X.; et al. Quantitative Intramolecular Singlet Fission in Bipentacenes. *J. Am. Chem. Soc.* **2015**, *137*, 8965−8972.

(14) Zirzlmeier, J.; Lehnherr, D.; Coto, P. B.; Chernick, E. T.; Casillas, R.; Basel, B. S.; Thoss, M.; Tykwinski, R. R.; Guldi, D. M. Singlet Fission in Pentacene Dimers. *Proc. Natl. Acad. Sci. U. S. A.* **2015**, *112*, 5325−5330.

(15) Gough, T.; Mengel, M.; Rowntree, P.; Scoles, G. Infrared Spectroscopy at the Surface of Clusters: SF6 on Ar. *J. Chem. Phys.* **1985**, *83*, 4958−4961.

(16) Müller, M.; Izadnia, S.; Vlaming, S. M.; Eisfeld, A.; LaForge, A.; Stienkemeier, F. Cooperative Lifetime Reduction of Single Acene Molecules attached to the Surface of Neon Clusters. *Phys. Rev. B: Condens. Matter Mater. Phys.* **2015**, *92*, 121408.

(17) Nijegorodov, N.; Ramachandran, V.; Winkoun, D. The Dependence of the Absorption and Fluorescence Parameters, the Intersystem Crossing and Internal Conversion Rate Constants on the Number of Rings in Polyacene Molecules. *Spectrochim. Acta, Part A* **1997**, *53*, 1813−1824.

(18) May, V. Kinetic Theory of Exciton-Exciton Annihilation. *J. Chem. Phys.* **2014**, *140*, 054103.

(19) Burdett, J. J.; Müller, A. M.; Gosztola, D.; Bardeen, C. J. Excited State Dynamics in Solid and Monomeric Tetracene: The Roles of Superradiance and Exciton Fission. *J. Chem. Phys.* **2010**, *133*, 144506.

(20) Wilson, M. W. B.; Rao, A.; Johnson, K.; Gélinas, S.; di Pietro, R.; Clark, J.; Friend, R. H. Temperature-Independent Singlet Exciton Fission in Tetracene. *J. Am. Chem. Soc.* **2013**, *135*, 16680−16688.

(21) Zhang, B.; Zhang, C.; Wang, R.; Tan, Z.; Liu, Y.; Guo, W.; Zhai, X.; Cao, Y.; Wang, X.; Xiao, M. Nonlinear Density Dependence of Singlet Fission Rate in Tetracene Films. *J. Phys. Chem. Lett.* **2014**, *5*, 3462−3467.

(22) Förster, T. 10th Spiers Memorial Lecture. Transfer Mechanisms of Electronic Excitation. *Discuss. Faraday Soc.* **1959**, *27*, 7−17.

(23) Jang, S. Generalization of the Foerster Resonance Energy Transfer Theory for Quantum Mechanical Modulation of the Donor-Acceptor Coupling. *J. Chem. Phys.* **2007**, *127*, 174710.

(24) Marciniak, H.; Pugliesi, I.; Nickel, B.; Lochbrunner, S. Ultrafast Singlet and Triplet Dynamics in Microcrystalline Pentacene Films. *Phys. Rev. B: Condens. Matter Mater. Phys.* **2009**, *79*, 235318.

(25) Stienkemeier, F.; Meier, F.; Lutz, H. Spectroscopy of Barium attached to Superfluid Helium Clusters. *Eu. Phys. J. D* **1999**, *9*, 313−315.

(26) Dvorak, M.; Müller, M.; Knoblauch, T.; Bünermann, O.; Rydlo, A.; Minniberger, S.; Harbich, W.; Stienkemeier, F. Spectroscopy of 3, 4, 9, 10-Perylenetetracarboxylic Dianhydride (PTCDA) Attached to Rare Gas Samples: Clusters vs. Bulk Matrices. I. Absorption Spectroscopy. *J. Chem. Phys.* **2012**, *137*, 164301.

(27) Pentlehner, D.; Riechers, R.; Dick, B.; Slenczka, A.; Even, U.; Lavie, N.; Brown, R.; Luria, K. Rapidly Pulsed Helium Droplet Source. *Rev. Sci. Instrum.* **2009**, *80*, 043302.

DOI: 10.1021/acs.jpclett.7b00319
J. Phys. Chem. Lett. 2017, 8, 2068−2073

(28) Hagena, O. Condensation in Free Jets: Comparison of Rare Gases and Metals. *Z. Phys. D: At., Mol. Clusters* **1987**, *4*, 291−299.
(29) Buck, U.; Krohne, R. Cluster Size Determination from Diffractive He Atom Scattering. *J. Chem. Phys.* **1996**, *105*, 5408−5415.
(30) Wörmer, J.; Guzielski, V.; Stapelfeldt, J.; Möller, T. Fluorescence Excitation Spectroscopy of Xenon Clusters in the VUV. *Chem. Phys. Lett.* **1989**, *159*, 321−326.
(31) Gomez, L. F.; Loginov, E.; Sliter, R.; Vilesov, A. F. Sizes of Large He Droplets. *J. Chem. Phys.* **2011**, *135*, 154201.
(32) Farges, J.; Deferaudy, M. F.; Raoult, B.; Torchet, G. Structure and Temperature of Rare-Gas Clusters in a Supersonic Expansion. *Surf. Sci.* **1981**, *106*, 95−100.
(33) Klots, C. E. Temperatures of Evaporating Clusters. *Nature* **1987**, *327*, 222−223.
(34) Dvorak, M.; Müller, M.; Bünermann, O.; Stienkemeier, F. Size Dependent Transition to Solid Hydrogen and Argon Clusters Probed via Spectroscopy of PTCDA Embedded in Helium Nanodroplets. *J. Chem. Phys.* **2014**, *140*, 144301.
(35) Inokuchi, H.; Akamatu, H. Electrical Conductivity of Organic Semiconductors. *Solid State Phys.* **1961**, *12*, 93−148.
(36) De Kruif, C. Enthalpies of Sublimation and Vapour Pressures of 11 Polycyclic Hydrocarbons. *J. Chem. Thermodyn.* **1980**, *12*, 243−248.

DOI: 10.1021/acs.jpclett.7b00319
J. Phys. Chem. Lett. 2017, 8, 2068−2073